Co−C Bond Reactivity and *Cis* Influence Relationship in Benzylcobaloximes with Glyoxime and Dimesitylglyoxime

Mouchumi Bhuyan, Moitree Laskar, Debaprasad Mandal, and B. D. Gupta*

Department of Chemistry, Indian Institute of Technology, Kanpur, 208 016, India

Received April 12, 2007

Benzyl cobaloximes, $ArCH_2Co(dioxime)_2Py$, with two different dioximes, glyoxime (gH) and dimesitylglyoxime (dmestgH), have been synthesized and characterized by ^1H and ^{13}C NMR and UV−vis spectroscopy. The dioxy adducts, $ArCH_2(O_2)Co(dioxime)_2Py$, were prepared by the insertion of molecular oxygen into the Co−C under photochemical conditions. The rate of insertion depends upon the nature of the dioxime and follows the order dmestgH ≫ dpgH > chgH > dmgH > gH. The steric *cis* influence of the dioximes on the Co−C bond also follows the same order. The study also suggests that the interactions between the axial benzyl group and the dioximes have significant influence on the Co−C bond reactivity. Such interactions are also seen in the molecular structure of $[C_6H_4CH_2Co(gH)_2$-(4-^{t}BuPy)] and in the dioxy complexes 4-CN-$C_6H_4CH_2(O_2)Co(dmestgH)_2Py$ and 2-naphthylCH_2-$(O_2)Co(dmestgH)_2Py$. On the basis of the results we have supported the cage mechanism for the oxygen insertion into the Co−C bond.

Introduction

One of the unique and intriguing properties of the coenzyme B_{12} is different catalytic activity of two different coenzymes. How the Co−C bond is activated toward homolysis or heterolysis is an enduring subject of research.[1,2] The recent crystallographic data on cobalamins suggest that the structural effects of changes in "R" are similar to those found in the cobaloximes, $RCo(dmgH)_2B$, and sometimes can be related to their chemical reactivity.[2] [Cobaloximes have the general formula $RCo(L)_2B$, where R is an organic group σ-bonded to cobalt. B is an axial base *trans* to the organic group, and L is a monoanionic dioxime ligand (e.g., glyoxime (gH), dimethylglyoxime (dmgH), 1,2-cyclohexanedione dioxime (chgH), diphenylglyoxime (dpgH), and dimesitylglyoxime (dmestgH)).] Since the Co−C bond cleavage is the key step involved in B_{12}-dependent enzymatic or cobaloxime-mediated reactions, the strength of the Co−C bond as a function of steric and electronic factors with a wide range of axial ligands in cobaloximes and in the related complexes with different chelates has been systematically investigated.[2] The Co−C bond length indeed responds to the steric rather than electronic effect in the organocobaloximes.[2] The bond lengths in structurally characterized complexes vary over a remarkably broad range of 0.2 Å from methyl to adamantyl cobaloximes.[3] Spectroscopic evidence has been presented that even longer bonds occur in more sterically hindered systems, which have thus far proved to be too unstable for X-ray structural characterization.[4] The results, based on spectral and structural studies, have shown that, in addition to the *trans* effect of the axial base, the *cis* influence of the equatorial dioxime on the axial ligands has significant effect toward the stability of the Co−C bond.[5−7] The inherently weak Co−C bond in the organocobaloximes shows homolytic cleavage with visible light similar to the activation of vitamin B_{12} by apoenzyme.[8] The insertion of molecular oxygen into the Co−C bond has extensively been used to test the reactivity of these compounds,[7] and its rate in the benzyl cobaloximes was found to follow the order dpgH > chgH > dmgH. The *cis* influence also has the same order.[7] Since the Co−C bond cleavage is the key step in these reactions and the effect of the *cis* influence is felt most on the Co−CH_2 bond, the question is if these two factors, *cis* influence and rate of insertion, are related to each other in some way.

Since the cobaloximes with dimesitylglyoxime (dmestgH) show the highest steric *cis* influence among the known dioximes [dmestgH > dpgH > chgH > dmgH > gH],[5] we have synthesized the benzyl cobaloximes with glyoxime and dimesitylglyoxime—the two extreme cases—and studied their insertion reaction with molecular oxygen. The benzyl system is particularly chosen because of the inherently weak Co−C bond and the weak interaction between the benzyl group and the dioxime may influence the Co−C bond reactivity especially because these have been shown to slow down the Co−C and C−Ph bond rotation.[9] In order to see the influence of these interactions on the Co−C bond stability/reactivity, we have measured and compared the rate data with the alkyl analogues where such interactions are lacking. We have also studied the

* Corresponding author. E-mail: bdg@iitk.ac.in. Tel: +91-512-2597046. Fax: +91-512-2597436.

(1) Brown, K. L. *Dalton Trans.* **2006**, 1123.
(2) Randaccio, L. *Comments Inorg. Chem.* **1999**, *21*, 327.
(3) (a) Randaccio, L. *Inorg. Chem.* **1983**, *22*, 3416, and references therein. (b) Bresciani-Pahor, N.; Marzilli, L. G.; Randaccio, L.; Summers, M. F.; Toscano, P. J. *Coord. Chem. Rev.* **1985**, *63*, 1. (c) Randaccio, L.; Bresciani-Pahor, N.; Zangrando, E.; Marzilli, L. G. *Chem. Soc. Rev.* **1989**, *18*, 225.
(4) (a) Gupta, B. D.; Vijaikanth V.; Singh, V. *Organometallics* **2004**, *23*, 2069. (b) Randaccio, L.; Bresciani-Pahor, N.; Toscano, P. J. Marzilli, L. G. *J. Am. Chem. Soc.* **1981**, *103*, 6347. (c) Trommel, J. S.; Warncke, K.; Marzilli, L. G. *J. Am. Chem. Soc.* **2001**, *123*, 3358. (d) Siega, P.; Randaccio, L.; Marzilli, P. A.; Marzilli, L. G. *Inorg. Chem.* **2006**, *45*, 3359.
(5) Mandal, D.; Gupta, B. D. *Organometallics* **2005**, *24*, 1501, and references therein.
(6) Gupta, B. D.; Qanungo, K. *J. Organomet. Chem.* **1997**, *543*, 125.
(7) (a) Gupta, B. D.; Vijaykanth, V.; Singh, V. *J. Organomet. Chem.* **1998**, *570*, 1. (b) Gupta, B. D.; Roy, M.; Das, I. *J. Organomet. Chem.* **1990**, *397*, 219.
(8) (a) Pratt, J. M.; Whitera, B. R. D. *J. Chem. Soc. A* **1971**, 252. (b) Ramakrishna, D. N.; Symons, M. C. R. *J. Chem. Soc., Faraday Trans. 1* **1984**, 423. (c) Jensen, F.; Madan, V.; Buchnan, D. H. *J. Am. Chem. Soc.* **1971**, *93*, 5285.
(9) (a) Mandal, D.; Gupta, B. D. *Organometallics* **2006**, *25*, 3305. (b) Mandal, D.; Gupta, B. D. *Organometallics* **2007**, *26*, 658.

10.1021/om7003578 CCC: $37.00
Publication on Web 06/12/2007

Scheme 1. Benzyl Cobaloximes and Oxygen Insertion into the Co−C Bond

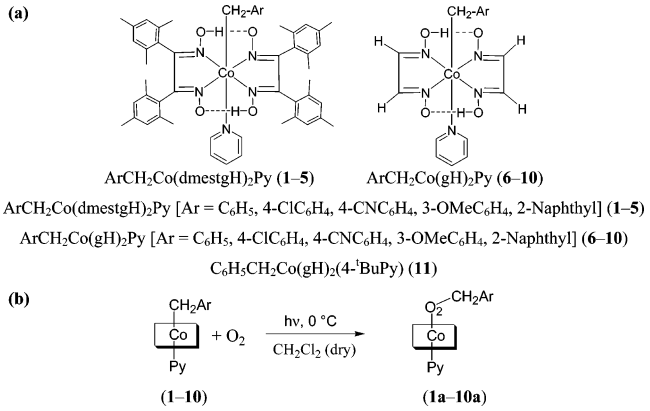

structural features of these oxygen-inserted complexes since there is no report of a crystal structure with $Co(O_2)$ bound to a primary carbon atom.[10]

Results and Discussion

Synthesis. Two series of complexes, $ArCH_2Co(dmestgH)_2Py$ (**1**−**5**) and $ArCH_2Co(gH)_2Py$ (**6**−**10**), have been synthesized (Scheme 1). All these complexes are new, and their elemental analysis data are given in Supporting Information Table S1.

$ClCo(dmestgH)_2Py$ was synthesized according to the procedure by Busch et al.[11] The preparation required the addition of Et_3N. However, when we tried to prepare it using the conventional procedure reported for $ClCo(dioxime)_2Py$ [dioxime = gH, dmgH, dpgH], we could get a maximum yield of 10%. The side product was EPR active and looked like a $[Co-(O_2)^{\bullet}]$ radical. No attempt was made to analyze this.

The synthesis of $ArCH_2Co(dmestgH)_2Py$ was accomplished according to the procedure previously established for the alkyl cobaloximes.[5] Ethanol is a better solvent than methanol, and a large excess of ethanol and 10-fold excess of $NaBH_4$ were essential; otherwise the yield was poor. The workup must be carried out rapidly under an argon atmosphere since the Co−C bond is highly sensitive toward oxygen; otherwise the product is contaminated with the oxygen-inserted product. For example, a solution of **3** and **5** kept for crystallization in air gave the crystal of the oxygen-inserted products **3a** and **5a**, respectively. The gH complexes (**6**−**10**) were synthesized by a general procedure detailed earlier for $RCo(gH)_2Py$. The workup procedure was similar to that described in our recent papers; the addition of acetic acid during workup is essential to compensate for the loss of the acidic gH proton in the basic medium.[10b]

Oxygen Insertion: General Comments. The insertion of oxygen is free radical nonchain in nature and shows general characteristics as found in earlier studies; for example, (a) the reaction does not proceed in the dark at 0 °C, (b) the reaction stops as soon as the irradiation is stopped, and (c) the reaction is inhibited by the free radical trap galvinoxyl. The best temperature for the reaction is 0 °C, though it proceeds at ambient temperature also. The reaction follows a first-order kinetics. The overall order of reaction is 2, i.e., first order with respect to both the complex and oxygen.[7a]

Spectroscopy: Characterization of these Complexes. The *cis* and *trans* influence in alkyl cobaloximes, $RCo(dioxime)_2Py$ (dioxime = gH, dmgH, chgH, dpgH, dmestgH), have already been discussed in detail in our previous publications.[5,6,12] We therefore will highlight only the salient features in the present complexes.

The complexes were preliminary characterized by ^1H and ^{13}C NMR spectroscopy, and the spectral data for **1**−**10** and **1a**−**10a** have been tabulated in Tables 1−4. The ^1H NMR spectra are easily assigned on the basis of their chemical shifts. The signals are assigned according to their relative intensities and are consistent with the literature values on the corresponding alkyl cobaloximes. Since no ^{13}C NMR has been reported for any oxygen-inserted cobaloxime, we have assigned the values keeping in view the chemical shifts in the parent complexes.

We have recently observed that the interaction between the axial and equatorial dioxime ligand affects the structure, Co−C bond reactivity, and NMR chemical shifts in benzyl cobaloximes; namely, such interactions cause restriction of Co−C and/or C−Ph rotation at subzero temperature and are partly responsible for the nonequivalence of dioxime and CH_2 protons in 2-substituted benzyl cobaloximes, $2\text{-}XC_6H_4CH_2Co(dioxime)_2Py$ [dioxime = dmgH, dpgH, and gH].[9] The crystal structures of benzyl cobaloximes support this; the benzyl group always lies over one of the dioxime wings and has π-interaction with the dioxime ring current. Such interactions have considerably affected the structure of pyrazine-bridged dicobaloximes; the alkyl complex attains the staggered conformation, whereas the benzyl analogue acquires the eclipsed conformation.[13] The same type of π-interaction between the axial and equatorial ligand has been reported by Randaccio et al.[14] in $RCo(DBPh_2)_2B$ and Stynes et al.[15] in $LFe^{II}(DBPh_2)L'$, where this interaction defines the ligand's orientation.

A reactivity difference toward oxygen in the benzyl and alkyl cobaloximes, $RCo(dmestgH)_2Py$, has also been observed; the benzyl complex gives the oxygen-inserted product, whereas the alkyl analogues give air-stable Co(II).[16]

Such interactions play a key role and affect the chemical shifts of the mesityl group in **1**−**5** in comparison to the alkyl derivatives.[5,17] The *ortho*-methyl groups in free $dmestgH_2$ are equivalent and appear at δ 2.14 ppm, whereas these are nonequivalent and the methyl at the 2-position is highly shielded by the ring current of the axial pyridine in alkyl or benzyl complexes and appears at around 1.45 ppm. The chemical shift of 6-Me depends on the nature of the axial R group; it is significantly shifted upfield and appears at 1.98 ppm in the benzyl (**1**) as compared to 2.19 ppm in the methyl analogue. This upfield shift is even larger in 2-naphthylcobaloxime (**5**). This is due to the interaction of the ring current of the benzyl or 2-naphthyl group with the dioxime. The 4-Me group is not

(10) (a) Giannotti, C.; Fontaine, C.; Chiaroni, A.; Riche, C. *J. Organomet. Chem.* **1976**, *113*, 57. (b) Chiaroni, A.; Pascard-Billy, C. *Bull. Soc. Chim. Fr.* **1973**, 781. (c) Alcock, N. W.; Golding, B. T.; Mwesigye-Kibende, S. *J. Chem. Soc., Dalton Trans.* **1985**, 1997.

(11) Lance, K. A.; Goldsby, K. A.; Busch, D. H. *Inorg. Chem.* **1990**, *29*, 4537.

(12) Gupta, B. D.; Yamuna, R.; Singh, V.; Tewari, U. *Orgnometallics* **2003**, *22*, 226.

(13) Mandal, D.; Gupta, B. D. *J. Organomet. Chem.* **2005**, *690*, 3746.

(14) (a) Dreos, R.; Tauzher, G.; Vuano, S.; Asaro, F.; Pellizer, G.; Nardin, G.; Randaccio, L.; Geremia, S. *J. Organomet. Chem.* **1995**, *505*, 135. (b) Asaro, F.; Dreos, R.; Geremia, S.; Nardin, G.; Pellizer, G.; Randaccio, L.; Tauzher, G.; Vuano, S. *J. Organomet. Chem.* **1997**, *548*, 211. (c) Dreos, R.; Geremia, S.; Nardin, G.; Randaccio, L.; Tauzher, G.; Vuano, S. *Inorg. Chim. Acta* **1998**, *272*, 74.

(15) (a) Stynes, D. V.; Leznof, D. B.; de Silva, D. G. A. H. *Inorg. Chem.* **1993**, *32*, 3989. (b) Stynes, D. V. *Inorg. Chem.* **1994**, *33*, 5022. (c) Vernik, I.; Stynes, D. V. *Inorg. Chem.* **1996**, *35*, 6210, and references therein.

(16) Mandal, D.; Bhuyan, M.; Laskar, M.; Gupta, B. D. *Organometallics* **2007**, *26*, 2795−2798.

(17) Mandal, D.; Chadha, P.; Laskar, M.; Bhuyan, M.; Gupta, B. D. *Tetrahedron Lett.* **2007**, *48*, 2377.

Table 1. ^{1}H NMR Data for 1−5 and 1a−5a at Room Temperature in $CDCl_3$

	ligand (dmestgH)					pyridine				
	Me (2)	Me (4)	Me (6)	aromatic	CH_2	α	*β*	*γ*	O−H···O	aromatic/others
1	1.45	2.15	1.98	6.58, 6.68	3.55	8.97	7.36	7.84	18.83	7.06(t), 7.16(t), 7.56(d)
1a	1.52	2.17	2.04	6.62, 6.70	4.71	8.75	a	7.84	19.10	7.16−7.36(m)
2	1.45	2.15	1.98	6.58, 6.70	3.45	8.94	7.36	7.84	18.80	7.02(d), 7.48(d)
2a	1.52	2.17	2.04	6.62, 6.72	4.66	8.73	7.26	7.85	19.08	7.22(d), 7.11(d)
3	1.44	2.16	1.98	6.60, 6.71	3.41	8.91	7.37	7.86	18.77	7.33(d), 7.61(d)
3a	1.54	2.18	2.01	6.63, 6.72	4.74	8.73	7.34	7.85	19.08	7.48(d), 7.42(d)
4	1.45	2.14	2.00	6.58, 6.69	3.53	8.96	7.36	7.84	18.79	6.96(t), 7.15(d), 3.74 (OMe)
4a	1.52	2.18	2.05	6.61, 6.70	4.69	8.75	7.33	7.83	19.10	6.83−7.07(m), 3.72 (OMe)
5	1.45	2.13	1.83	6.57, 6.63	3.72	8.98	*c*	*c*	18.91	7.95−7.26(m)
5a	1.53	2.16	2.01	6.65, 6.62	4.88	8.76	7.34	7.85	19.15	7.37−7.76(m)
1b[a]	1.52	2.18	2.48	6.62, 6.80	4.62	8.67	*c*	7.70	18.68	7.25−7.29(m)
1c[b]	1.51	2.19	2.24	6.63, 6.77	3.50	8.72	7.33	7.85		

[a] **1b** = $PhCH_2(SO_2)Co(dmestgH)_2Py$. [b] **1c** = $Me(O)_2Co(dmestgH)_2Py$. [c] Merge with aromatic.

Table 2. ^{1}H NMR Data for 6−10 and 6a−10a at Room Temperature in $CDCl_3$

			pyridine				
	CH_2 (s)	gH	α (d)	*β* (t)	*γ* (t)	aromatic/others	O−H···O
6	3.01	7.24	8.54	7.35	7.75	7.11−7.05(m)	17.67
6a	4.42	7.56	8.34	7.31	7.75	6.93(d), 7.24(d)	17.72
7	2.92	7.26	8.51	7.35	7.75	7.00(d), 7.12(d)	17.65
7a	4.36	7.57	8.32	7.30	7.75	7.19−7.22(m)	
8	2.87	7.28	8.47	7.35	7.77	6.99(d), 7.32, 7.29, 7.11(d)	17.37
8a	4.47	7.59	8.32	7.31	7.77	7.37(d), 7.55(d)	17.66
9	3.00	7.25	8.54	7.35	7.77	6.66−6.80(m), 6.93−7.00(m), 3.79 (OMe)	17.63
9a	4.40	7.57	8.34	7.31	7.75	6.79(d), 6.85(d), 7.17(t), 3.76 (OMe)	17.74
10	3.18	7.21	8.55	7.34	7.75	7.40−7.69(m)	17.74
10a	4.59	7.53	8.33	7.35	7.72	7.41−7.44(m) 7.76−7.81(m)	17.68

Table 3. ^{13}C NMR Data for 1−5 and 1a−5a at Room Temperature in $CDCl_3$

		pyridine					
	C═N (dmestgH)	α	*β*	*γ*	aromatic/others	Me (dmestgH)	CH_2
1	153.27	151.32	124.87	138.39	138.67, 138.15, 137.06, 130.10, 128.56, 128.44, 128.29, 126.32, 124.96	20.94, 20.53, 20.37	32.79
1a	154.90	152.04	125.02	139.18	138.64, 136.67, 131.60, 128.99, 128.69, 128.15, 126.14	21.06, 20.17, 19.95	76.89
2	153.42	151.55	124.94	138.50	146.54, 139.07, 138.83, 137.99, 137.04, 131.23, 128.63, 128.48, 128.36, 126.19	20.97, 20.47, 20.36	31.38
2a	154.80	152.02	125.01	139.06	138.84, 136.64, 130.64, 128.83, 128.64, 128.33, 128.07, 127.83, 126.22	21.04, 20.26, 19.90	77.44
3	153.80	151.33	125.04	138.68	154.97, 139.03, 137.80, 137.04, 132.06, 130.44, 129.23, 128.68, 128.47, 126.01, 107.66, 120.19 (CN)	21.00, 20.45, 19.93	30.37
3a	154.89	152.02	125.02	139.17	138.63, 136.66, 131.60, 128.99, 128.68, 128.14, 126.13,	21.05, 20.16, 19.95	
4	153.35	151.35	124.90	138.40	149.46, 138.69, 138.17, 137.04, 128.56, 128.29, 126.35, 159.71, 138.98, 129.24, 122.66, 114.67, 111.78, 55.22 (OMe)	20.97, 20.55, 20.37	32.71
4a	154.78	152.05	125.00	138.94	125.31, 126.29, 127.14, 127.44, 128.05, 128.65 132.80, 133.18, 134.69, 136.63, 55.03 (OMe)	21.04, 20.27, 19.92	78.49
5	154.08	152.05	125.25	*c*	139.24, 138.97, 136.63, 133.18, 129.11, 128.87, 128.06, 127.50, 126.75, 126.47	21.06, 20.26, 19.92	38.07
5a	154.78	152.05	125.00	138.94	136.63, 134.69, 133.18, 132.80, 128.65, 128.05, 127.44, 127.14, 126.29, 125.31	21.04, 20.27, 19.92	78.49
1b[a]	156.44	151.55	124.87	139.90	148.49, 139.36, 136.77, 135.71, 131.43, 129.18, 128.22, 128.13, 127.56, 125.86	21.01, 20.84, 20.33	65.18
1c[b]	154.59	151.98	125.00	139.08	138.84, 136.71, 128.72, 128.10, 126.27	19.88, 20.27, 21.10	65.79

[a] **1b** = $PhCH_2(SO_2)Co(dmestgH)_2Py$. [b] **1c** = $Me(O)_2Co(dmestgH)_2Py$. [c] Merge with aromatic.

affected at all and appears at the same chemical shift in the alkyl and benzyl complexes (Supporting Information Figures S1 and S2).

The crystal structure of $MeCo(dmestgH)_2Py$ shows that both the axial positions are very much crowded and laterally compressed by the four methyl groups of the equatorial dmestgH ligand.[5] Due to this steric crowding, pyridine is puckered (strained) and the axial methyl has an interaction with the 6-Me group (∼2.47 Å) (Supporting Information Figure S3). Any substitution on the axial methyl will further increase the steric crowding and lead to a higher bending angle (α), which in turn pushes 2-Me closer to pyridine. This is due to the *cis* influence of the dioxime on the Co−C bond. In the absence of the crystal structure we cannot confirm the increase in the bending angle; however its effect is clearly visible in the ^{1}H NMR chemical shifts of 2-Me. For example, on increasing the alkyl chain length from R = Me to Et, Pr, or benzyl, the 2-Me is upfield shifted from 1.51 to 1.45 ppm.

The effect of the *π*-interaction is also seen in the gH complexes; gH protons in **6**−**10** are upfield shifted (*δ* 7.24 ppm)

Table 4. ^{13}C NMR Data for 6−10 and 6a−10a at Room Temperature in $CDCl_3$

		pyridine				
	C═N (gH)	α	*β*	*γ*	aromatic	CH_2
6	138.00	149.88	125.57	*a*	138.31, 128.67, 127.71, 124.98	
6a	140.09	150.75	125.68	138.82	136.35, 129.54, 128.76, 128.03, 127.73	78.34
7	138.10	149.89	125.62	138.05	144.26, 130.31, 129.79, 127.84	
7a	140.14	150.79	125.75	138.91	134.99, 133.59, 130.86, 128.24	77.48
8	138.31	149.81	125.75	*a*	152.37, 132.41, 131.41, 107.59, 120.19 (CN)	32.29
8a	140.15	150.73	125.76	138.97	133.89, 129.53, 128.56, 107.01, 120.08 (CN)	
9	138.11	149.87	125.58	*a*	159.09, 147.07, 128.50, 121.38, 113.23, 111.47, 55.13 (OMe)	34.47
9a	140.10	150.76	125.69	138.83	137.86, 128.99, 121.74, 114.48, 113.88, 55.17 (OMe)	78.27
10	138.08	149.95	125.62	138.03	137.95, 128.34, 127.25, 126.86, 125.92, 125.87, 124.62	
10a	140.15	150.71	125.70	138.84	133.96, 133.16, 128.35, 127.98, 127.51, 127.19, 126.58, 126.18, 125.52	78.36

[a] Merge with CN(gH).

as compared to the reported alkyl analogues (δ 7.42 ppm). Thus, the benzyl or 2-naphthyl ring must attain a proper orientation to show a π-interaction with the dioxime ring current. To perceive how important this requirement is, we have compared the chemical shifts of **1**−**5** with the $PhCH_2(O_2)Co(dmestgH)_2$-Py and $Bn(SO_2)Co(dmestgH)_2Py$ complexes since the orientation of the benzyl group varies significantly in these complexes (see later).[18]

Important differences are noticed when the chemical shifts of dmestgH complexes (**1**−**5**) are compared with the gH complexes (**6**−**10**); for example, CH_2 is highly downfield shifted (0.5−0.6 ppm) in **1**−**5** as compared to the value in **6**−**10**. A similar trend is observed for Py_α and O−H···O also. This is due to the higher cobalt anisotropy of dmestgH complexes. $\Delta\delta$-(^{13}C, C═N) is a good measure of the cobalt anisotropy as observed in many cobaloximes; the higher the value, the higher the cobalt anisotropy.[5] [Instead of δ^{13}C(C═N), the $\Delta\delta$(^{13}C, C═N) value has been taken. This is to avoid the direct effect of the substituent on the δ(C═N) value. $\Delta\delta$(^{13}C, C═N) represents the field effect (combined effect of cobalt anisotropy and ring current) and is equal to $\delta_{complex} - \delta_{free\ ligand}$ (see ref 5 for details).] The present results also support this; $\Delta\delta$(^{13}C, C═N) is 8−9 ppm higher in **1**−**5** as compared to complexes **6**−**10**. A comparison with the other benzylCo(dioxime)$_2$Py complexes gives the *cis* influence order of the dioximes as dmestgH > dpgH > chgH ≈ dmgH > gH (Supporting Information Table S2). The same order was also observed in alkylCo(dioxime)$_2$Py complexes.[5,6,12]

Comparison of 1−10 with 1a−10a. Incorporation of dioxygen into the Co−C bond affects the chemical shift of RCH_2, Py_α, and the dioxime in the ^{1}H and ^{13}C NMR spectra of **1a**−**10a**. RCH_2 is directly attached to O_2 and hence shifts highly downfield by 1.1−1.4 ppm (and about 74 ppm in ^{13}C NMR). A higher magnitude of $\Delta\delta$(^{13}C, C═N) [1.5−2.0 ppm] in **1a**−**10a** as compared to **1**−**10** points to the higher cobalt anisotropy in the dioxy complexes. The pyridine resonance is affected in a similar way. A comparison of $\Delta\delta$(^{1}H, Py_α) gives useful information.

The coordination shift of Py_α is affected both by cobalt anisotropy and by the ring current of the dioxime, and both operate in the opposite directions.[5,19] The net value depends upon the interplay of these two factors; in the gH complexes the ring current effect is more than the cobalt anisotropy, and the reverse is true in the dmestgH complexes. The data show that $\Delta\delta$(^{1}H, Py_α) in **1a**−**10a** is upfield shifted as compared to **1**−**10**, and it is 0.4 ppm downfield shifted in **1**−**5** as compared with **6**−**10**. A similar shift is observed when **1a**−**5a** is compared with **6a**−**10a**. The upfield shift of Py_α in **1a**−**10a** means the ring current contribution is more, and the downfield shift in **1**−**5** or **1a**−**5a** means the cobalt anisotropy contribution is more. The ring current effect is more in **1a**−**10a** because Py_α is closer to the dioxime ring (Co−N_{Py} bond length is slightly shorter than in organocobaloxime). The behavior is similar to the inorganic cobaloximes.

The insertion of O_2 affects the dioxime protons also. The gH protons shift downfield by 0.3 ppm in the dioxy complexes as compared to the parent cobaloximes due to higher cobalt anisotropy in the former. This is much larger compared to the shift in the dmgH (0.1 to ∼0.2 ppm)[7] and dmestgH complexes (0.02−0.1 ppm).

The effect of cobalt anisotropy is much more pronounced in the gH complexes since "H" is directly bonded to the dioxime, and it is one bond away in the dmgH complexes and is too far away in the dmestgH complexes.

Interestingly, the chemical shift of 2-Me is identical in MeO_2-$Co(dmestgH)_2Py$, $C_6H_5CH_2O_2Co(dmestgH)_2Py$, and $C_6H_5CH_2$-$SO_2Co(dmestgH)_2Py$ and is justified in view of the above discussion.[20] The crystal structures of the dioxy complexes show that the strain is released and the bending angle decreases (∼3°) with the result that 2-Me moves away from the pyridine ring (3.1 Å compared to 2.8 Å, see Figure 2).

Comparison with the SO_2-Inserted Complexes. A further change in conformation of the benzyl group occurs in C_6H_5-$CH_2SO_2Co(dioxime)_2Py$.[18] Here the benzyl group lies vertically up and perpendicular to the dioxime plane and is too far away to have any interaction with the dioxime protons. The ^{1}H NMR spectrum of $C_6H_5CH_2SO_2Co(dmestgH)_2Py$[17,20] should, therefore, be similar to that of $XCo(dmestgH)_2Py$. However, 6-Me is highly deshielded and the signal appears at δ 2.48 ppm. This is due to its interaction with the SO_2 group that lies close to it (Supporting Information Figure S2). A similar observation was made earlier in the corresponding gH and dmgH complexes;

(18) Chadha, P.; Mahata, K.; Gupta, B. D. *Organometallics* **2006**, *25*, 92.

(19) Gupta, B. D.; Yamuna, R.; Mandal, D. *Orgnometallics* **2006**, *25*, 706.

(20) $Me(O_2)Co(dmestgH)_2Py$ (^{1}H NMR; 400 MHz, $CDCl_3$): δ Py: α-*H* 8.72 (d, 2H, J = 5.2 Hz), *γ*-*H* 7.85 (t, 1H, J = 7.4 Hz), *β*-*H* 7.33 (t, 2H, J = 6.8 Hz); dmestgH(CH_3): 1.51 (s, 12H), 2.19 (s, 12H), 2.24 (s, 12H); dmestgH(*H*): 6.63 (s, 1H), 6.67 (s, 1H); $Co(O_2)CH_3$: 3.50 (s, 3H). $Bn(SO_2)Co(dmestgH)_2Py$ (^{1}H NMR; 400 MHz, $CDCl_3$): δ O−*H*···O: 18.68; Py: α-*H* 8.67 (d, 2H, J = 6.0 Hz), *γ*-*H* 7.70 (t, 1H, J = 8.0 Hz), *β*-*H* merge with aromatic; dmestgH(CH_3): 1.52 (s, 12H), 2.18 (s, 12H), 2.48 (s, 12H); dmestgH(*H*): 6.62 (s, 1H), 6.80 (s, 1H); $Co(O_2)CH_2$: 4.62 (s, 2H); aromatic: 7.25−7.29 (m).

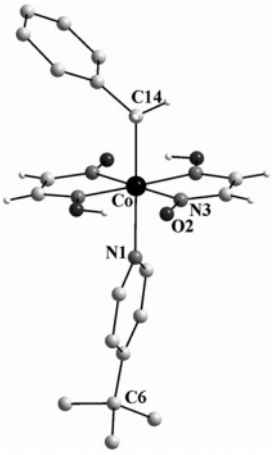

Figure 1. Molecular structure of **11**.

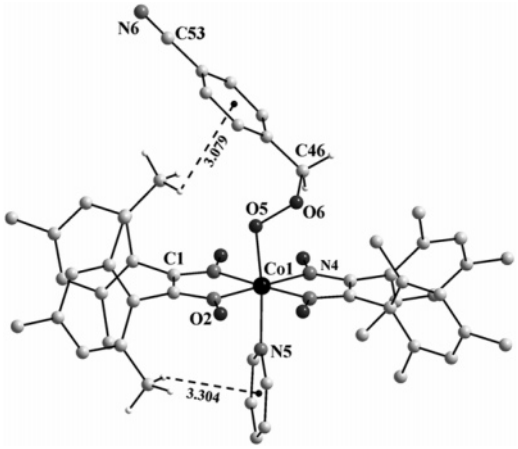

Figure 2. Molecular structure of **3a**.

for example, gH (or dmgH) protons appear at δ 7.24 (2.00) ppm in $C_6H_5CH_2Co(gH)_2Py$ and $C_6H_5CH_2Co(dmgH)_2Py$ and at δ 7.55 (2.30) ppm in $C_6H_5CH_2SO_2Co(gH)_2Py$ and $C_6H_5CH_2SO_2Co(dmgH)_2Py$.[12,18] However, unlike dmestgH, the downfield shift here is not due to the close proximity of the SO_2 group with the gH or dmgH(Me) protons, but it results mainly from the change in cobalt anisotropy. The gH or dmgH(Me) protons are close to the $[Co(dioxime)_2]^+$ moiety and are affected much more than the dmestgH(Me) protons.

X-ray Crystallographic Studies. Description of the Structure of $C_6H_5CH_2Co(gH)_2(4\text{-}^tBuPy)$ (11). The Diamond diagram of the molecular structure along with the numbering scheme is shown in Figure 1, and selected bond lengths and bond angles are given in Table 5. The geometry around the cobalt atom is distorted octahedral, with four nitrogen atoms of the dioxime (gH) in the equatorial plane. Benzyl and 4-^{t}BuPy are axially coordinated. 4-^{t}BuPy is coordinated to the cobalt atom with bending (C6−N1−Co1 172.65°), as observed in many crystal structures,[18,21] and the bending is due to the crystal-packing force. The benzyl group is located over the dioxime wing and shows some interaction with the dioxime moiety. Co−C/Co−N_{ax} distances (2.049(8)/2.051(6) Å) and Co−C−C/N−Co−C angles (119.7(5)/178.6(3)°) are almost identical with the other benzyl cobaloximes with dmgH as the equatorial ligand. The deviation of the cobalt atom from the mean equatorial N_4 plane (*d*) is +0.021 Å, the butterfly bending angle between two equatorial dioximes halves (α) is 2.54°, and

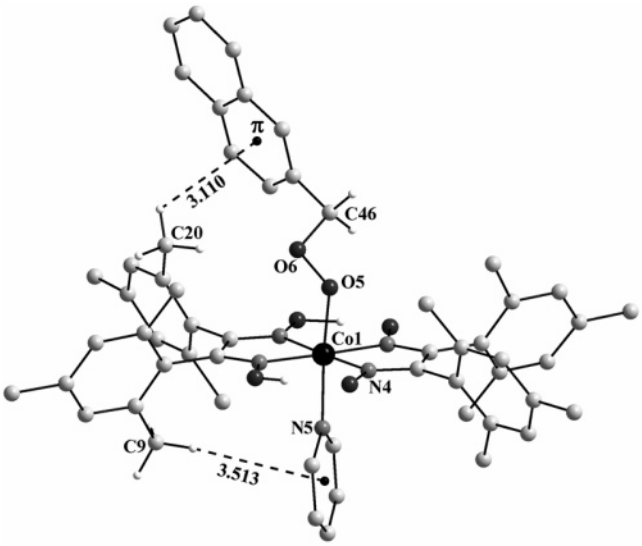

Figure 3. Molecular structure of **5a**.

the twist angle of the pyridine plane (τ) is 79.62°. [*d* is the deviation of the cobalt atom from the mean equatorial N_4 plane; the butterfly bending angle (α) is the dihedral angle between two dioxime planes, and τ is the torsion angle between two planes, axial base pyridine and the plane that bisects the dioxime C−C bonds through the cobalt atom. The positive sign of α and *d* indicates bending toward R and displacement toward base and *vice versa* (see ref 5 for details).] Interestingly, the Co−C (2.061(4) Å) and Co−N_{ax} (2.054(3) Å) distances, *d* (+0.02 Å), α (2.68°), and τ (74.36°) in 2-Br-$C_6H_4CH_2Co(gH)_2Py$ are very similar to the corresponding values in **11**.

Description of the Molecular Structures of 3a and 5a. A slow evaporation of solvent from the solution of **3a** and **5a** (dichloromethane, acetonitrile, benzene, and hexane) results in the formation of orange crystals. The X-ray data analysis of these crystals shows the composition as 4CN-$C_6H_4CH_2$-$(O_2)Co(dmestgH)_2Py\cdot 2CH_3CN\cdot C_6H_6$ (**3a**) and 2-naphthylCH_2-$(O_2)Co(dmestgH)_2Py\cdot 2CH_2Cl_2$ (**5a**). Diamond diagrams of the molecular structures for **3a** and **5a** along with selected numbering schemes are shown in Figures 2 and 3, respectively. Selected bond lengths and bond angles are given in Table 5. The O−O distances of 1.435/1.399 Å are similar to those in the reported peroxo cobaloxime complexes.

These are the first crystal structures of the oxygen-inserted cobaloximes with $Co(O_2)$ bound to a primary carbon atom. All three previously reported crystal structures have either a secondary or tertiary carbon bound to $Co(O_2)$ with dmgH as the equatorial ligand.[10] The geometry about the central cobalt is distorted octahedral with four nitrogen atoms of the dioxime in the equatorial plane and pyridine and the oxygen atom axially coordinated. A comparison of the molecular structure of **3a** with the reported cumyl$(O_2)Co(dmgH)_2Py$ (**X**$_1$)[10a] shows that the Co−N_{Py} and Co−O distances, the C−H···π interaction, and the orientation of the Bn−O−O group are almost identical. Interestingly, the benzyl group in $ArCH_2Co(dmgH)_2Py$[9] shows a similar orientation as well as a C−H···π interaction to that in **3a** and **5a**.

The R−O−O−R′ dihedral angle is a significant parameter for all the peroxides. The Co−O−O−C dihedral angles in **3a** and **5a** are strikingly similar to the reported alkylperoxycobaloximes. Evidently, the same minimization of lone pair−lone pair (LP−LP) interactions that governs the structure of hydrogen peroxide (dihedral angle 112°) is the dominant factor in **3a** and **5a**. The Co−O−O−C dihedral angle gives useful information

(21) (a) Galinkina, J.; Rusanov, E.; Wagner, C.; Schmidt, H.; Ströhl, D.; Tobisch S.; Steinborn, D. *Organometallics* **2003**, *22*, 4873.

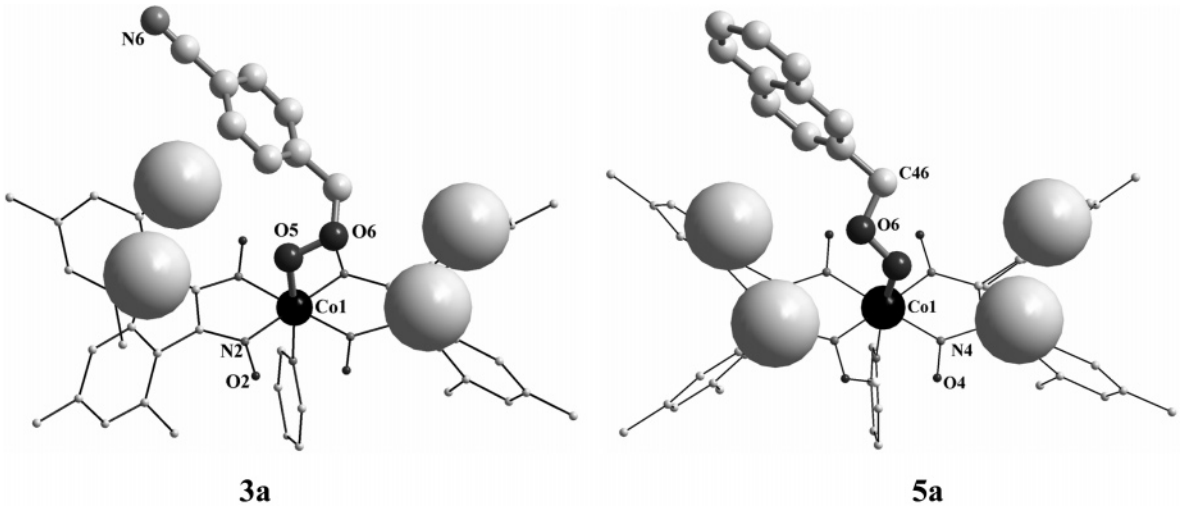

3a **5a**

Figure 4. Orientation of the $ArCH_2$ group over the cavity in the molecular structure of **3a** and **5a**.

Table 5. Selected Bond Lengths (Å), Bond Angles (deg), and Structural Data for 3a, 5a, and 11 and Comparison with Other Dioxy Complexes (X_1 = $C_6H_5(CH_3)_2C(O_2)Co(dmgH)_2Py$; X_2 = 4-Me-$C_6H_4(CH_3)CH(O_2)Co(dmgH)_2Py$; X_3 = $C_2H_5OOC(CH_2)_2(CH_3)CH(O_2)Co(dmgH)_2Py$)

	3a	**5a**	X_1	X_2	X_3	**11**
$Co-O_{ax}/C_{ax}$	1.896(2)	1.875(4)	1.897	1.898	1.923(4)	2.049(8)
$Co-N_{ax}$	1.995(3)	1.978(4)	1.994	2.013	2.007(5)	2.051(6)
O−O	1.435(3)	1.399(5)	1.454	1.456	1.415(7)	
O−C	1.421(4)	1.446(7)	1.461	1.449	1.428(8)	
Co−O−O/ Co−C−C	116.43(17)	116.5(3)	112.41	112.84	115.3(3)	119.7(5)
O−O−C	107.5(2)	108.1(4)	111.15	107.15	108.2(5)	
Co−O−O−C	106.2(2)	−114.0(4)	−131.57	−113.94	100.0(4)	
O−C−C	115.4(3)	105.3(5)	100.77	104.92	112.21	
O−O−C−C	60.8(4)	175.3(5)	172.34	164.36	63.66	
$N_{py}-Co-O_{ax}/C_{ax}$	173.80(11)	171.8(2)	175.25	176.88	177.97	178.6(3)
d (Å)	+0.011	+0.021	0.027	0.029	0.011	+0.023
α (deg)	3.17	3.14	6.91		3.17	2.54
τ (deg)	79.81	88.24	88.16		79.83	79.62
C−H···π	3.079(1)	3.110(2)	3.432			3.999(5)

about the bond pair−lone pair (BP−LP) and LP−LP repulsions around the O−O bond in such complexes; for example cumyl-$(O_2)Co(dmgH)_2Py$ (**X_1**), having the tertiary carbon bonded to $Co(O_2)$, has the highest value of −131.6°, whereas it is 100.0-(4)° in the reported *sec*-alkyl(O_2) complex (**X_3**).[10c] The higher the angle, the greater the BP−LP interaction. The C−O−O angle also gives similar information; the cumyl(O_2) complex (**X_1**) has the largest angle (111.1°) among the reported structures and has the maximum BP−LP interaction. Although $Co(O_2)$ is bound to a primary carbon in **3a** and **5a**, the dihedral angle suggests that the steric crowding by the dmestgH(Me) on the phenyl (or naphthyl) ring is more like the steric crowding between the tertiary carbon and the dioxime in **X_1**. Can this be the reason that the dmestgH complexes are more unstable than the corresponding dmgH complexes since the tertiary carbon bound to cobalt is much more unstable than the primary (in general, the Co−C bond stability follows the order 1° > 2° > 3°)? The steric interaction of the [Co(dioxime)$_2$] moiety with the axial ligand can also be inferred from the Co−O−O angle; it is much higher in the dmestgH complexes (**3a** and **5a**) than the dmgH complex (116° vs 112°). [We have not considered the comparison with the value of 115° in **X_3** since it lacks the interaction between the axial and the equatorial ligand.] This also suggests a higher steric *cis* effect of the dmestgH ligand than the dmgH.

There are a few important differences between the molecular structures of **3a** and **5a**; the displacement of cobalt atom (*d*) from the N_4 plane is toward pyridine in both **5a** and **3a**. The naphthyl ring is almost perpendicular to the dioxime plane in **5a**, whereas the benzyl ring is somewhat tilted in **3a**. This is why the O−CH_2−C angles are so different in **3a** and **5a** [115.4° and 105.3°]. However, the Co−O−O angle is almost the same [116.4° and 116.5°], indicating identical steric crowding due to the [Co(dmestgH)$_2$] moiety. The most striking difference lies in the O−O−C−C dihedral angle, which defines the orientation of the C−C bond of the benzyl or naphthyl group; for example, it drastically changes from 60.8° in **3a** to 175.3° in **5a**. This is explained as follows.

The 4-CN-$C_6H_4CH_2$− group in **3a** partly occupies the cavity created by four methyl groups of two dmestgH ligands. The phenyl ring is above the cavity and has interactions with the equatorial ligand (Figure 4). However, the bulkier 2-naphthyl group cannot fit into this cavity and undergoes inherent interaction with the dioxime from the sideways direction in such a way that it attains an orientation with a very large dihedral angle [the O−O and the C−C(Ph) plane are almost parallel (175°) to each other] (Figure 4). The cumyl(O_2) complex (**X_1**) also shows a similar orientation of the bulkier CH(Me)Ph with a large dihedral angle. Although the complex **X_3** bears a secondary carbon and lacks interaction with the dioxime, the axial group orients with a very small dihedral angle of 63.66°. This suggests that both the steric *cis* influence and the interactions between axial and equatorial ligands are important and contribute to the Co−C bond stability.

To summarize, the dmestgH ligand has the highest steric *cis* influence among all the reported complexes with other dioximes and $Co(O_2)$ though bound to a primary carbon in **3a** and **5a**,

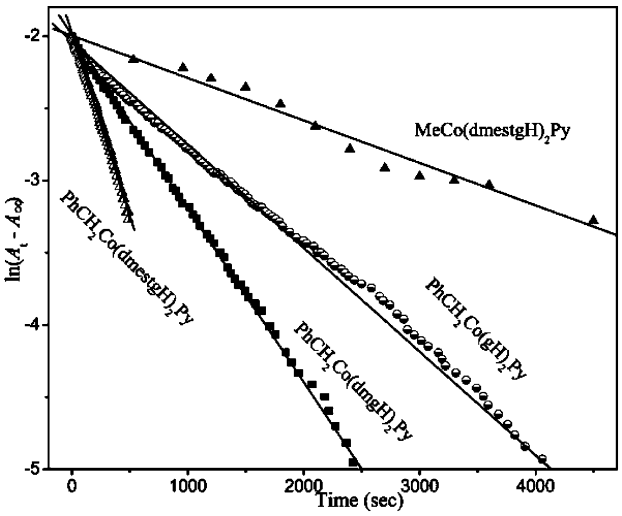

Figure 5. Comparison of the plot of $\ln(A_t - A_\infty)$ versus time (s) for $PhCH_2Co(gH)_2Py$ (**6**), $PhCH_2Co(dmgH)_2Py$, $PhCH_2Co(dmestgH)_2Py$ (**1**), and $CH_3Co(dmestgH)_2Py$.

Table 6. Pseudo-First-Order Rate Constants (k_{obs}) for Oxygen Insertion into the Co−C Bond in $RCo(dioxime)_2Py$

$RCo(dioxime)_2Py$	k_{obs} (s^{-1})
$PhCH_2Co(gH)_2Py$	7.1×10^{-4}
$PhCH_2Co(dmgH)_2Py$	1.2×10^{-3}
$PhCH_2Co(dpgH)_2Py$	4.8×10^{-3}
$PhCH_2Co(dmestgH)_2Py$	5.0×10^{-2}
n-$BuCo(dmestgH)_2Py$	4.5×10^{-4}
$MeCo(dmestgH)_2Py$	2.9×10^{-4}

and the steric crowding by the dmestgH methyl on the phenyl (or naphthyl) ring is more like the tertiary carbon in the dmgH complex.

Rate Studies. Kinetic Runs. The insertion reaction is usually carried out at 0 °C to avoid any side reactions due to thermal conditions. However it has been reported that the rate of insertion does not vary much between 0 and 25 °C.[7,22] We have, therefore, studied the rate of oxygen insertion in **1** and **6** at ambient temperature because of convenience only. In order to compare the data with the other dioximes, we have also carried out the rate studies in the corresponding dmgH and dpgH complexes under similar conditions. We have also confirmed that the rates (k_{obs}) do not vary much between 0 and 25 °C in these complexes. The Co−C CT band varies with the dioxime and occurs between 350 and 420 nm. So before starting the kinetic runs we have done a preliminary experiment to obtain the point where the largest change in absorbance occurs, and these are at 385, 363, and 390 nm for dmestgH, dmgH, and gH complexes, respectively. Ocean Optics software in the UV−vis machine allows continuous scan for the change in absorbance at a particular wavelength with time. The rate constants (k_{obs}) were calculated from the slope of the linear plots of $\ln(A_t - A_\infty)$, where A_t is the absorbance at time t and A_∞ is the final absorbance versus time (s), and are given in Figure 5 and Table 6. The rate data show that the insertion depends upon the equatorial ligand and follow the order dmestgH ≫ dpgH > dmgH > gH. The steric *cis* influence on the Co−C bond also follows the same order. We had observed the dependence of the rate of insertion on the *cis* influence in our earlier studies,[7a] but a conclusion could not be drawn from the data based only on the dmgH and dpgH complexes.

(22) Giannotti, C.; Fontaine, C.; Septe, B. *J. Organomet. Chem.* **1974**, *71*, 107.

Since the Co−C bond cleavage is the key step in the insertion reaction and the effect of the *cis* influence of the dioxime is felt most on the $Co-CH_2$ bond,[7a] the very high rate of insertion in the dmestgH complex is quite justified keeping in view the steric *cis* influence observed in the crystal structures. However, it is worth noting that the electronic *cis* influence for dpgH and dmestgH complexes is quite similar on the basis of the ^1H NMR data ($\delta(Co-CH_2)$ 3.55 ppm in both).

A reactivity difference in the oxygen insertion between alkyl and benzyl cobaloximes has been observed. In general, the benzyl complexes are more reactive than the alkyl complexes, although the Co−C bond length is similar in both. The steric *cis* influence of the methyl and benzyl group on the Co−C bond in the dmgH complexes, $RCo(dmgH)_2Py$, is found to be similar (α and *d* values are similar). However this is not the case in the dmestgH complexes; the steric *cis* influence is higher in the benzyl than the methyl [higher α value in the benzyl]. This is due to the steric crowding of the axial organic group by the 6-Me of dmestgH as observed in the ^1H NMR. Interestingly, on moving from methyl to any higher alkyl chain (C_2-C_4, ethyl to *n*-butyl), the steric *cis* influence of the dmestgH on the CH_2 group becomes similar to the benzyl cobaloxime.

In the recent study we have found that the Co−C bond homolysis in alkyl and benzyl cobaloximes, $RCo(dmestgH)_2Py$, leads to different product formation; the benzyl complex gives the oxygen-inserted product, whereas the alkyl derivative forms air-stable $Co^{II}(dmestgH)_2(Py)_2$.[16] The formation of Co^{II} as the end product in the alkyl cobaloxime points to its stabilization by the macrocyclic ligand. The oxygen-inserted product is formed in the benzyl case due to the stabilization of Co^{II} by the macrocyclic ligand and the formation of stable benzyl radical, which remains intact inside the cage by the interaction with the macrocyclic ligand. This leads to a buildup of the persistent radicals in solution and steers the reaction in a highly selective manner. The very fact that the dioxy complex is formed indicates that the benzyl group is in the vicinity of the reaction center [$Co^{II}(O_2)$]. This can be seen as a cage effect. However, there is a possibility that the difference in reactivity may partly arise due to the difference in the stability of the benzyl and alkyl radicals. This reactivity difference is similar to that in the AdoCbl and MeCbl.

So a comparison of the rate data in these complexes would be of interest. The k_{obs} is 2.9×10^{-4}, 4.5×10^{-4}, and 5.0×10^{-2} s^{-1} for Me, *n*-Bu, and $BnCo(dmestgH)_2Py$; the rate is much higher in the benzyl than in the alkyl complexes. Also these rates are much higher than in the corresponding dmgH complexes (see Table 6). The difference in the rates between the benzyl and alkyl must be due to the additional interaction between the axial and the equatorial ligand. The k_{obs} in the gH complex **6** is the smallest among all the dioxime complexes and fits well into the *cis* influence order given above.

The different product formations and the difference in rate in the *n*-butyl and benzyl complexes suggest that not only the Co−C bond reactivity is different but the recombination step also has an influence on the oxygen insertion rate and the formation of $Bn(O_2)$ is facilitated by the persistent radical effect (cage efficiency) of the benzyl radical.[16] This is similar to the difference in the Ado and MeCbl. Interestingly, the interaction between the axial and equatorial ligands (plausible cage mechanism Scheme 2) has also had a significant influence on the product yield in the insertion reaction; for example it is much lower (40%) in the butyl than in the benzyl analogue (80%).

The X-ray structure details also give useful information. In general, *d* is positive, α is low, and τ is ∼90° in MeCo-

Scheme 2. Plausible Cage Effect Mechanism of Oxygen Insertion Reaction

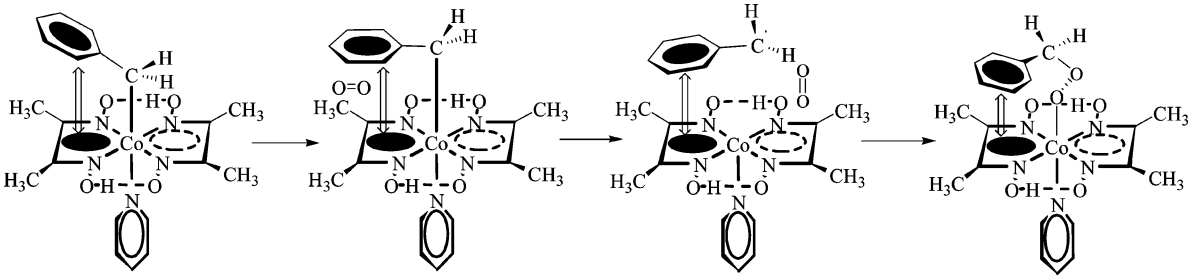

(dioxime)$_2$B (gH, dmgH, dpgH) (Supporting Information, Table S3). In contrast, *d* is negative, α is high, and *τ* is highly deviated from 90° in the dmestgH complex, MeCo(dmestgH)$_2$Py.[5] Its crystal structure also shows that the Py ring is puckered and has steric interaction with the 2-Me groups of dmestgH. The corresponding benzyl complexes are highly unstable in solution and suggest more strain in these molecules. The ^{1}H NMR has already shown that the 2-Me protons are more upfield shifted in the benzyl complex as compared to the methyl analogue due to its higher interaction with the pyridine ring current. This is possible if the bending angle of the dioxime is high, which will push the 2-Me groups closer to pyridine. The insertion of oxygen releases this strain and leads to lesser puckering of the dioxime. This is why a much smaller upfield shift of 2-Me in the oxygen-inserted product is observed. The low value of α (3.17° and 3.14°) and *d* (+0.011/+0.021 Å) in **3a** and **5a** supports this view. The release of strain might be the driving force for the higher rate constant for the O_2 insertion reaction in the dmestgH complexes, so much so that the otherwise less reactive alkyl analogues undergo facile oxygen insertion; for example the MeCo(dmestgH)$_2$Py complex goes to half completion and then attains an equilibrium state after 2 h, and the *n*-butyl complex goes to completion in 2 h.

Conclusion

The steric *cis* influence affects the Co−C bond stability/reactivity, and a good relationship has been found between the rate of oxygen insertion and the steric *cis* influence in benzyl cobaloximes. Both follow the same order dmestgH > dpgH > chgH > dmgH > gH. In addition to the steric *cis* influence of the dioximes, the interactions between the axial and equatorial ligands also play a significant role in the Co−C bond stability/reactivity and in the product formation. Such interactions are also present in the molecular structures of the dioxy complexes. The results support the cage mechanism for the insertion of oxygen in these complexes. Since the steric *cis* influence of the mixed dioxime complexes fall between the parent cobaloximes, it would be interesting to study the rate of oxygen insertion in the mixed dioxime complexes. However, complications will arise because these complexes equilibrate in solution to a mixture of products.

Experimental Section

General Comments. Cobalt chloride hexahydrate (SD Fine, India), glyoxime (Alfa Aesar, Lancaster), benzyl chloride, 4-chlorobenzyl chloride, 3-methoxybenzyl chloride, and 2-chloromethylnaphthalene were purchased from either Aldrich or Fluka and were used as such. Dichloroglyoxime,[11] dimesitylglyoxime,[11] ClCo(dioxime)$_2$Py (dioxime = glyoxime[12] and dimesitylglyoxime[5]), and 4-cyanobenzyl bromide[23] were prepared according to literature procedures. Silica gel (100−200 mesh) and distilled solvents were used in all reactions and chromatographic separations. ^{1}H and ^{13}C NMR spectra were recorded on a JEOL JNM Lambda 400 FT NMR instrument (at 400 MHz for ^{1}H and at 100 MHz for ^{13}C NMR spectra) in $CDCl_3$ solution with TMS as internal reference. Elemental analysis was carried out using a thermoquest CE instruments CHNS-O elemental analyzer. UV−vis spectra were recorded on an Ocean Optics USB4000 (BASi, USA) UV−vis spectrometer in dry chloroform.

X-ray Structural Determination and Refinement. Orange crystals were obtained by slow evaporation of the solvent (dichloromethane/acetonitrile/benzene/hexane) for **3a** and **5a** (in a methanol/dichloromethane mixture for **11** [$C_6H_4CH_2Co(gH)_2(4\text{-}^tBuPy)$]). Single-crystal X-ray data were collected using graphite-monochromated Mo Kα radiation (λ = 0.71073 Å) on a Bruker SMART APEX CCD diffractometer at 100 K for **3a** and **5a** and the data collected at 293 K on a CAD4 for **11**. The linear absorption coefficients, scattering factors for the atoms, and anomalous dispersion corrections were taken from *International Tables for X-ray Crystallography*.[24a] The data integration and reduction were processed with SAINT[25] software. An empirical absorption correction was applied to the collected reflections with SADABS[26] using XPREP.[27] The structures were solved by the direct method using SIR-97[28] and were refined on F^2 by the full-matrix least-squares technique using the SHELXL-97[24b] program package. All non-hydrogen atoms were refined anisotropically. The hydrogen atoms of the OH group of oxime were located on difference maps and were constrained to those difference map positions. The hydrogen atom positions or thermal parameters were not refined but were included in the structure factor calculations. The pertinent crystal data and refinement parameters are compiled in Table 7.

The cif files have been deposited with the Cambridge Crystallographic Data Centre (CCDC numbers for **11**, **3a**, and **5a** are 265406, 607226, and 634745). Copies of the data can be obtained free of charge from the Director, CCDC, 12 Union Road, Cambridge CB2, 1EX, U.K. (fax: +44-1223-336033; e-mail: deposit@ccdc.cam./ac.uk; or www: http://www.ccdc.cam.ac.uk/).

Synthesis of ArCH$_2$Co(dioxime)$_2$Py (1−10). The compounds **1**−**5** were synthesized by the general procedure detailed earlier for the synthesis of RCo(dmestgH)$_2$Py (where R is an alkyl group) and involved the reaction of Co^I with organic halide in ethanol (yield = 85−90%).[5] The compounds **6**−**10** were synthesized and purified by the procedure used for the synthesis of benzylCo(gH)$_2$Py; the addition of 2 or 3 drops of acetic acid was necessary during workup (yield 45−65%).[8b]

(23) (a) Tcheou, F.-K.; Shih, Y.-T.; Lee, K.-L. *J. Chin. Chem. Soc.* **1950**, *17*, 150. (b) Grice, R.; Owens, L. N. *J. Chem. Soc.* **1963**, 1947.

(24) (a) *International Tables for X-ray Crystallography*; Kynoch Press: Birmingham, England, 1974; Vol. IV. (b) Sheldrick, G. M. *SHELXL-97: Program for Crystal Structure Refinement*; University of Göttingen; Göttingen, Germany, 1997.

(25) *SAINT+*, 6.02 ed.; Bruker AXS: Madison, WI, 1999.

(26) Sheldrick, G. M. *SADABS, Empirical Absorption Correction Program*; University of Göttingen: Göttingen, Germany, 1997.

(27) *XPREP*, 5.1 ed.; Siemens Industrial Automation Inc.: Madison, WI, 1995.

(28) Altomare, A.; Burla, M. C.; Camalli, M.; Cascarano G. L.; Giacovazzo, C.; Guagliardi, A.; Moliterni, A. G. G.; Polidori, G.; Spagna, R. *J. Appl. Crystallogr.* **1999**, *32*, 115.

Table 7. Crystal Data and Structure Refinement Details for 3a, 5a, and 11

	3a·$2CH_3CN$·C_6H_6	**5a**·$2CH_2Cl_2$	**11**
empirical formula	$C_{63}H_{69}N_8O_6Co_1$	$C_{58}H_{64}Cl_4N_5O_6Co_1$	$C_{20}H_{26}Co_1N_5O_4$
fw	1093.19	1127.87	459.39
temp (K)	100(2)	100(2)	293(2)
diffrn measurement device/scan method	Smart CCD area detector/$\varphi-\omega$	Smart CCD area detector/$\varphi-\omega$	Enraf-Nonius CAD4 Mach2/$\theta-2\theta$
cryst syst	triclinic	monoclinic	monoclinic
space group	$P\bar{1}$	$P2_1$	$P2_1/n$
unit cell dimens			
a (Å)	14.2170(11)	8.6212(6)	10.177(4)
b (Å)	14.3381(11)	26.734(2)	10.854(4)
c (Å)	16.6229(13)	13.5996(10)	19.864(7)
α (deg)	112.352(2)	90	90
β (deg)	95.690(2)	102.9950(10)	101.0(2)
γ (deg)	111.594(2)	90	90
V (Å^3)	2799.0(4)	3054.2(4)	2153.9(14)
Z	2	2	4
ρ(calcd) (Mg/m^3)	1.297	1.226	1.417
μ(mm^{-1})	0.367	0.506	0.833
F(000)	1156	1180	960
cryst size (mm^3)	0.28 × 0.22 × 0.20	0.24 × 0.22 × 0.15	0.21 × 0.16 × 0.14
index ranges	$-18 \le h \le 18$, $-14 \le k \le 19$, $-21 \le l \le 22$	$-11 \le h \le 9$, $-35 \le k \le 34$, $-11 \le l \le 17$	$0 \le h \le 12$, $0 \le k \le 12$, $-23 \le l \le 23$
no. of reflns collected	18 867	14 960	4014
no. of indep reflns	13 342	10 776	3786
GOF on F^2	1.043	0.928	1.005
final R indices ($I > 2\sigma(I)$)	R1 = 0.0748, wR2 = 0.1987	R1 = 0.0667, wR2 = 0.1441	R1 = 0.0801, wR2 = 0.1430
R indices (all data)	R1 = 0.1041, wR2 = 0.2195	R1 = 0.851, wR2 = 0.1515	R1 = 0.1879, wR2 = 0.1836
no. of data/restraints/params	13 342/0/717	10 776/1/677	3786/0/271

Molecular Oxygen Insertion in $RCH_2Co(dioxime)_2Py$ (1−10): General Procedure.[7] A solution of $ArCH_2Co(dioxime)_2Py$ (0.07 g) in 15 mL of dichloromethane was irradiated at 0 °C with 2 × 200 W tungsten lamps at approximately 10 cm distance, and oxygen was bubbled through the solution. The progress of the reaction was monitored with TLC on silica gel using a 20% ethylacetate/CH_2Cl_2 mixture for **1**−**5** and 100% ethyl acetate for **6**−**10**. The reaction was complete in 1 h. There was a distinct color change from yellow-orange to dark brown at this stage. At the end of reaction, the solvent was evaporated and the crude product was purified on a silica gel column using ethyl acetate and CH_2Cl_2 as the eluent. Yield: 80−83% for **1a**−**5a** and 70−80% for **6a**−**10a**.

Kinetic Study. The kinetics study of the oxygen insertion in $ArCH_2Co(dioxime)_2Py$ under photochemical conditions was followed spectrophotometrically at 0 °C as well as at ambient temperature under pseudo-first-order conditions. Oxygen was bubbled through the solution and hence used in large excess. The progress of the reaction was monitored following the changes (decreases) in absorbance (the absorbance due to the Co−C CT band) at regular intervals. The k_{obs} rate constants were obtained from the slope of the linear plots of $\ln(A_t - A_\infty)$, versus time, where A_t is the absorbance at time t and A_∞ is the final absorbance. Kinetic data were analyzed with ORIGIN 6.1.

Acknowledgment. We thank DST (SR/S1/IC-12/2004) and CSIR [01(1949)/04/EMR II], New Delhi, India, for financial support.

Note Added after ASAP Publication: References 16 and 17 have been corrected. The paper was published on the Web on June 12, 2007. The corrected version was reposted on June 15, 2007.

Supporting Information Available: Table of CHN analysis data and molecular structure comparison data, representative figures of ^1H and ^{13}C NMR and UV−vis spectra, and CIF files for X-ray crystal structures of **11**, **3a**, and **5a**. This material is available free of charge via the Internet at http://pubs.acs.org.

OM7003578